Stirred-tank Batch Adsorption Test Fig. 4.9

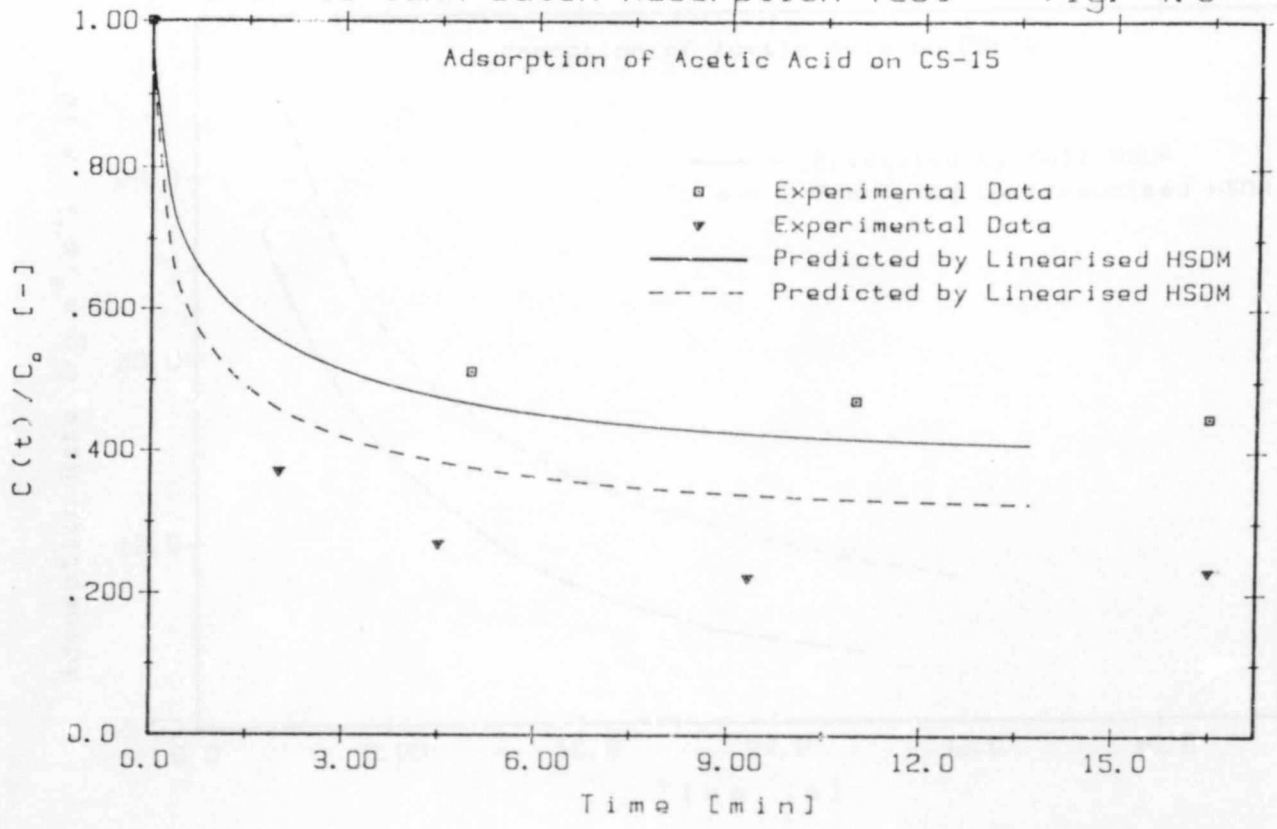

Stirred-tank Batch Adsorption Test Fig. 4.10

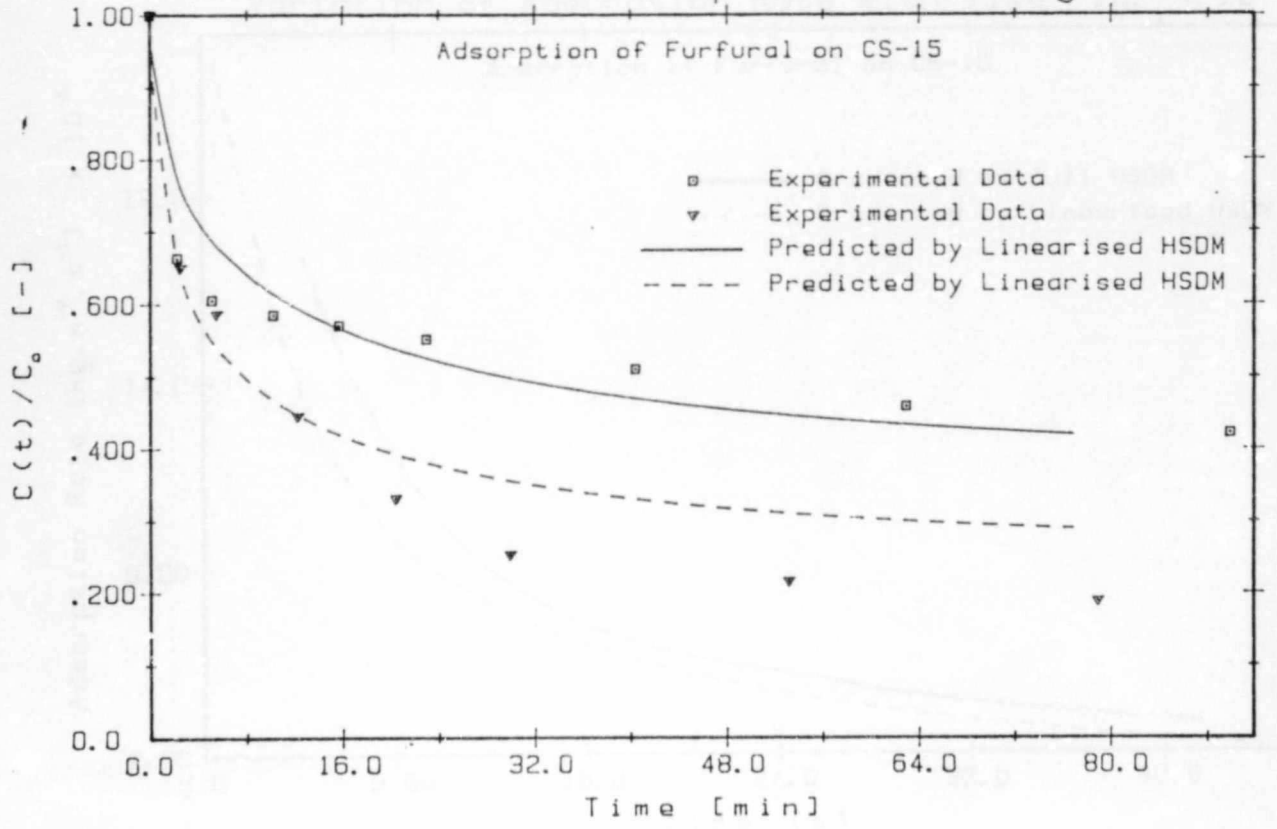

Variation of Adsorption Rate with Time Fig. 4.11

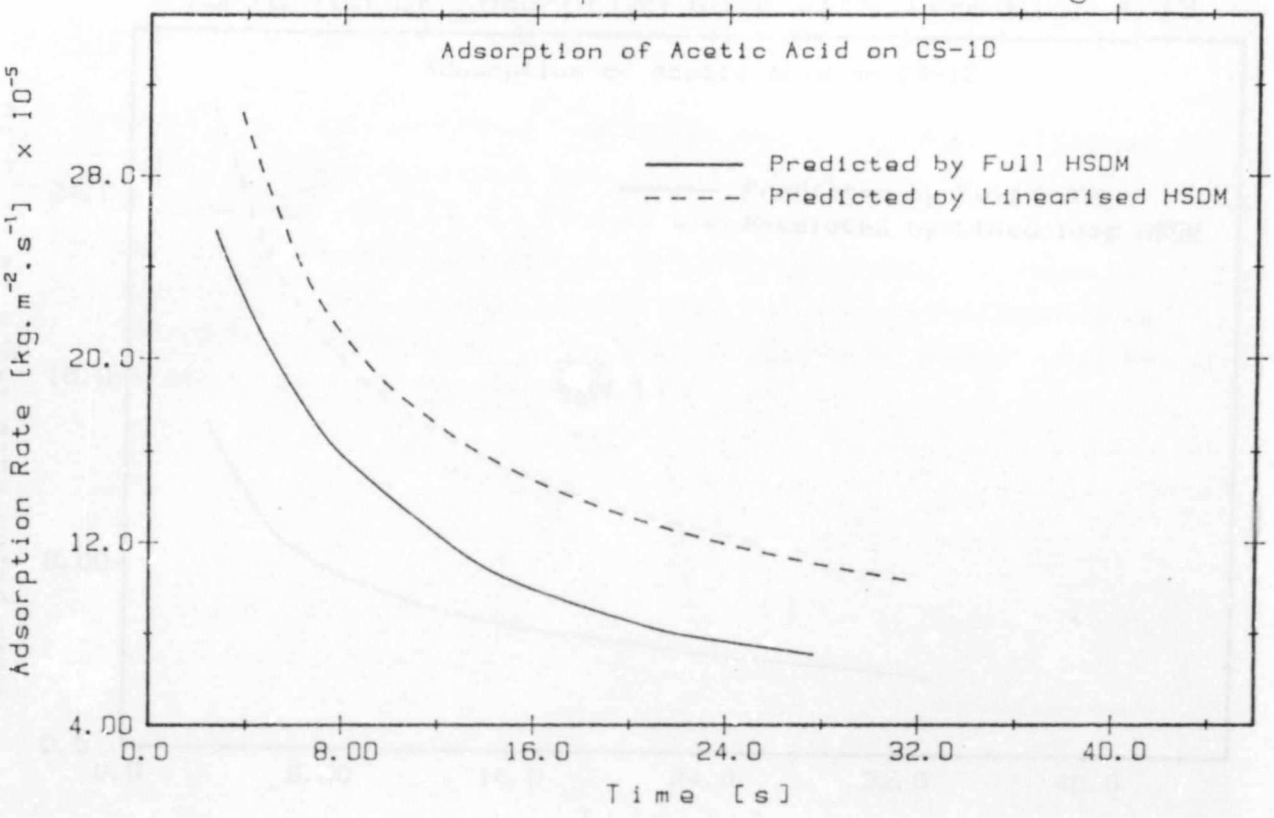

Variation of Adsorption Rate with Time Fig. 4.12

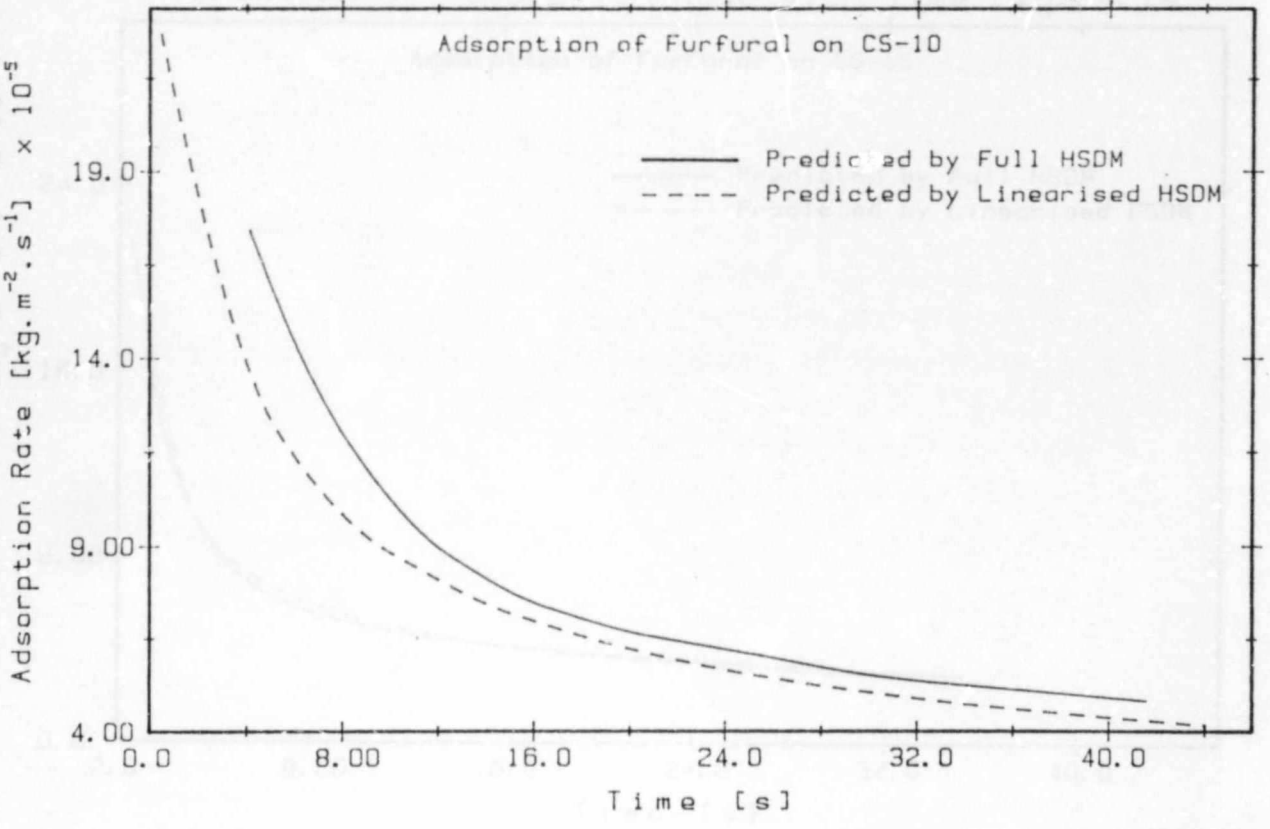

Variation of Adsorption Rate with Time Fig. 4.13

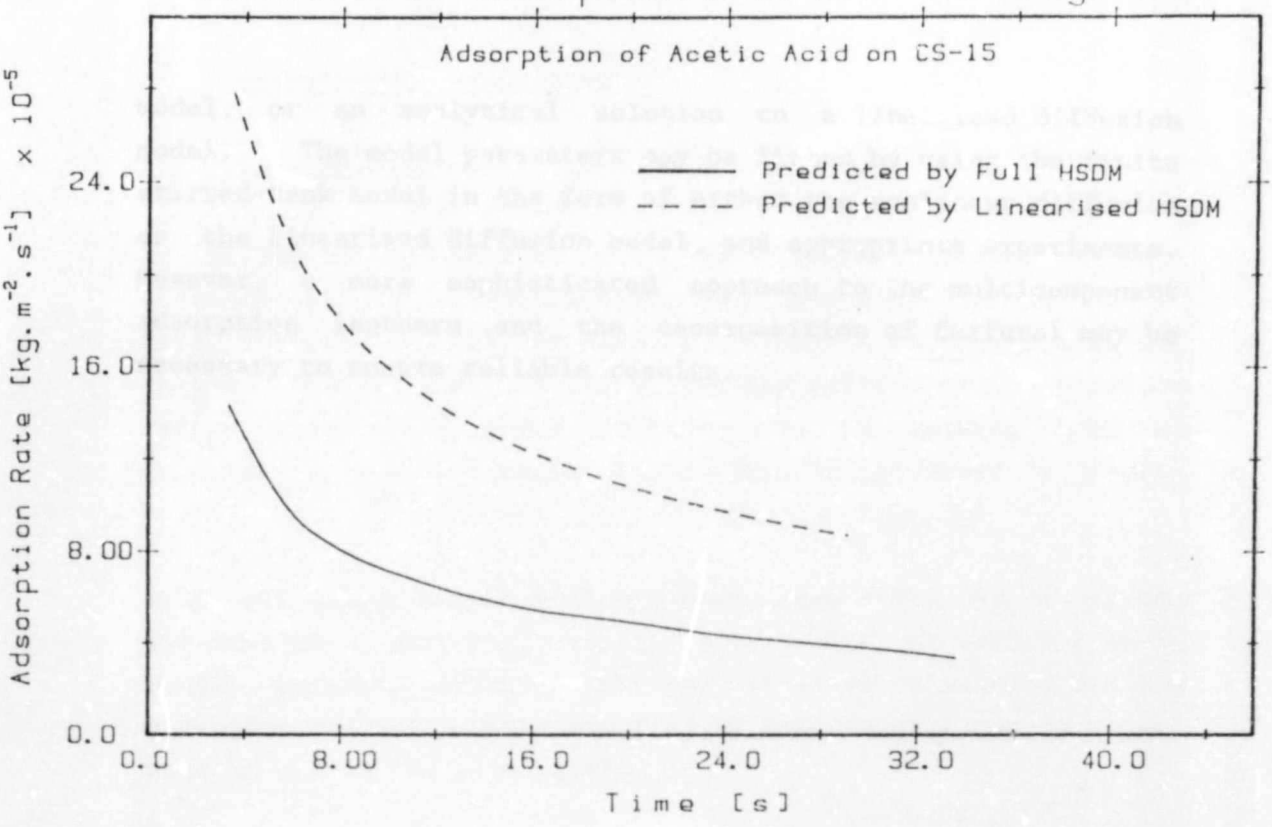

Variation of Adsorption Rate with Time Fig. 4.14

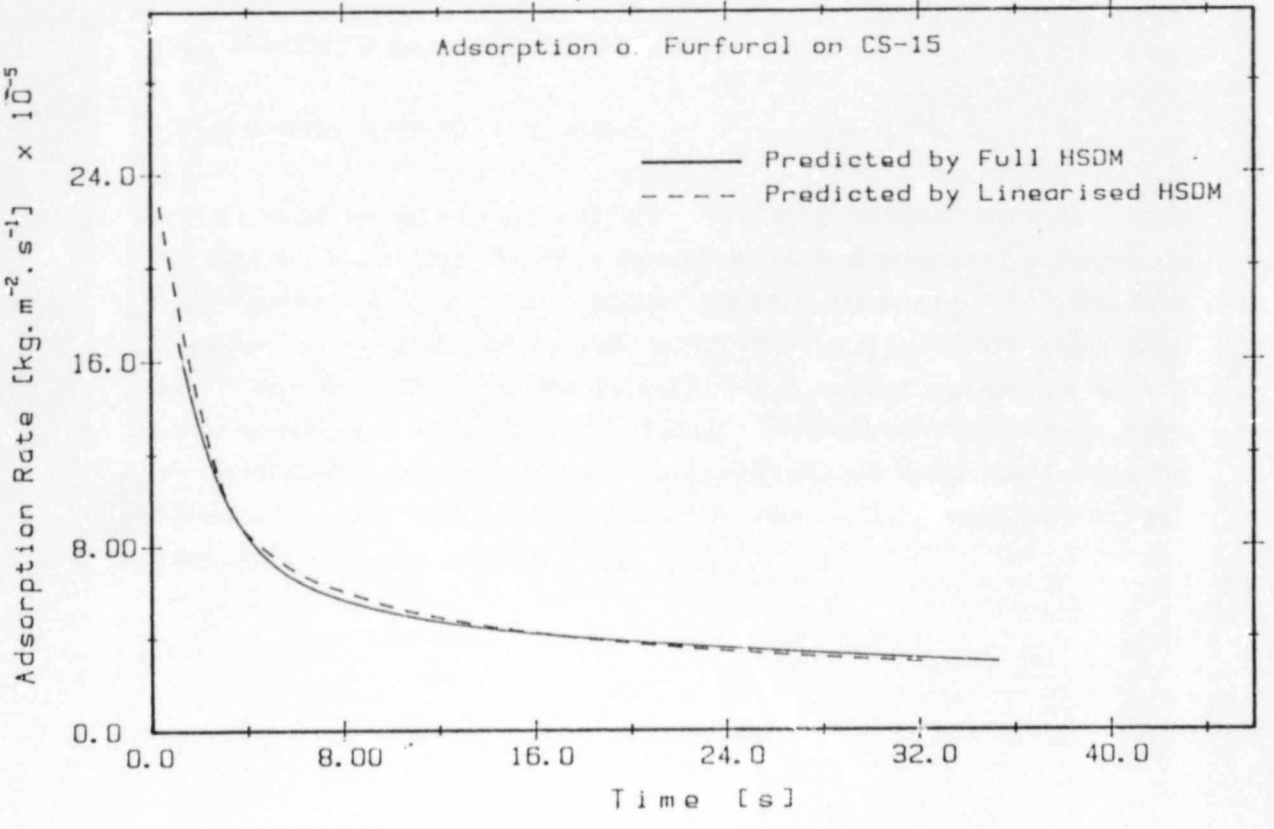

model, or an analytical solution to a linearised diffusion model. The model parameters may be fitted by using the finite stirred-tank model in the form of either the nonlinear diffusion or the linearised diffusion model, and appropriate experiments. However, a more sophisticated approach to the multicomponent adsorption isotherm and the decomposition of furfural may be necessary to ensure reliable results.

5 EXPERIMENTAL TECHNIQUES

5.1 Introduction

As discussed in section 1.1, the effluent system has been approximated as a solution of three components, namely acetic acid, furfural and sulphur dioxide. It has been stated that the sulphur dioxide was included for its effects on the solution rather than as a third component to be removed from the solution. The motivation behind this is discussed in section 2.2

Thus all experimental work was done using either of two pseudo one-component mixtures, namely acetic acid, or furfural in an acidic aqueous solvent. The concentration of sulphur dioxide was measured only at the start of an experimental run to ensure that it was at the right level.

The techniques employed in the various experimental measurements are discussed below.

5.2 Concentration Determination

5.2.1 Acetic acid determination

Acetic acid in an acidic sulphur dioxide solution was determined by first titrating the test solution into a measured aliquot of 0.05 molar I_2 to the iodine endpoint to convert the sulphur dioxide to iodic acid and sulphuric acid. The resulting solution was then titrated with 0.1 M sodium hydroxide to the phenolpthalein end-point to finally determine acetic acid. The concentration of acetic acid was calculated from the following formula - see APPENDIX III for reaction stoichiometry and derivation of the formula.

$$[CH_3COOH] = \left(\frac{0.1 \times V_{NaOH} - 0.2 \times V_I}{V_{Sample}} \right) \times 60.0 \quad \ldots(5/1)$$

Where V_{NaOH} = volume of sodium hydroxide required to reach the phenolpthalein endpoint [l]

V_I = volume of the standardised iodine aliquot, 0.025 l in this work [l]

V_{Sample} = volume of acetic acid/sulphur dioxide solution required to reach iodine endpoint [l]

$[CH_3COOH]$ = concentration of acetic acid [g/l]

This titrimetric method was found to fall far short of the modest accuracy required for this work.

At a later stage a liquid chromatograph became available, and acetic acid was determined by anion-exchange chromatography. The advantage of such an instrument was that it could also be used to determine acetate in a sodium hydroxide solution, as well as the simultaneous determination of furfural and acetic acid in mixtures. Such determinations were required in the elementary regeneration studies, and in experimental testing of theoretically derived multicomponent adsorbtion isotherms - see section 2.5.

The liquid chromatograph output was calibrated on the basis of peak height - see APPENDIX III for details and calibration data. Janik (1975) has reported the accuracy of this method to be comparable to that of peak-area calibration for the case of symmetrical peaks. A calibration curve is shown in Fig.5.1, and sample chromatograms are shown in Fig.5.2. Note that the acetic acid peak is symmetrical.

These chromatographic determinations were far more accurate than the titrimetric method discussed above, as well as far less time-consuming. Determination of acetic acid and furfural in

HPLC Calibration Curve

Fig. 5.1

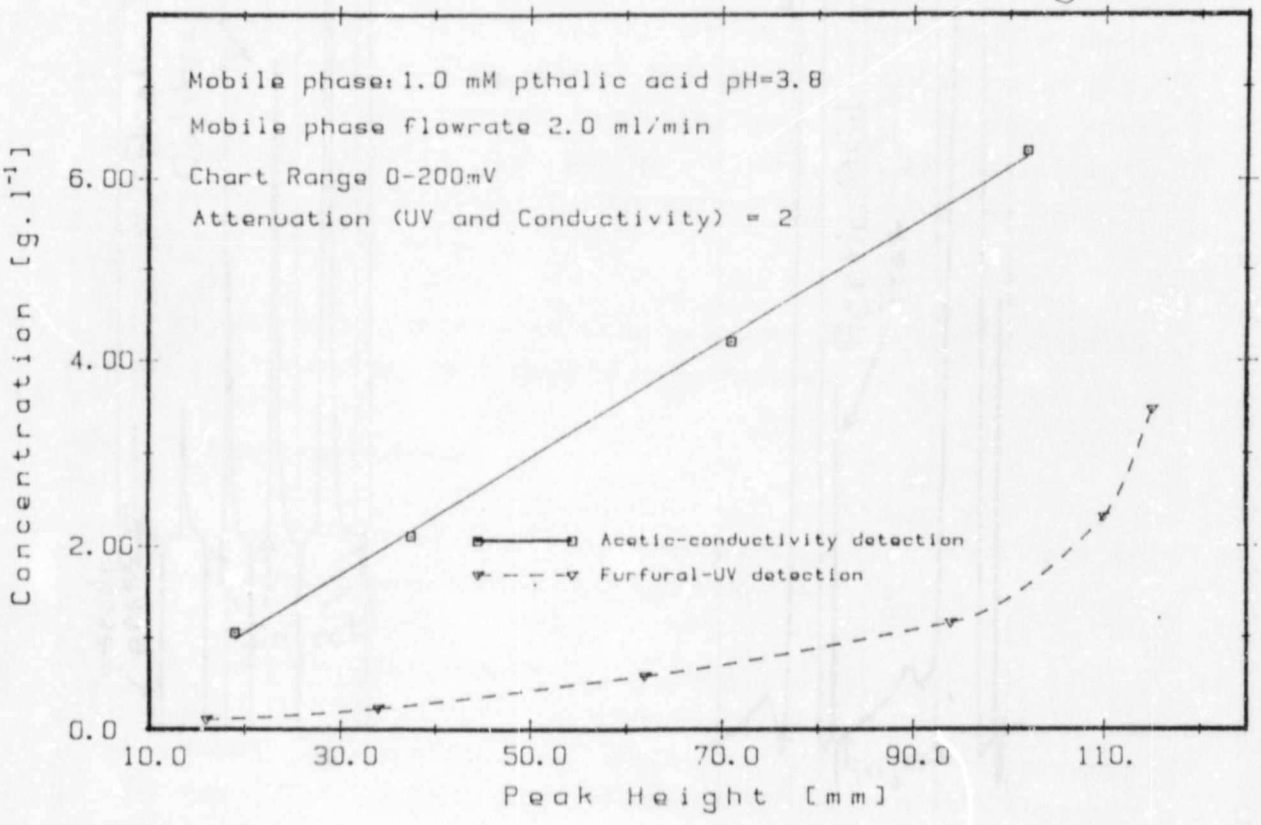

Sample Liquid-chromatograms

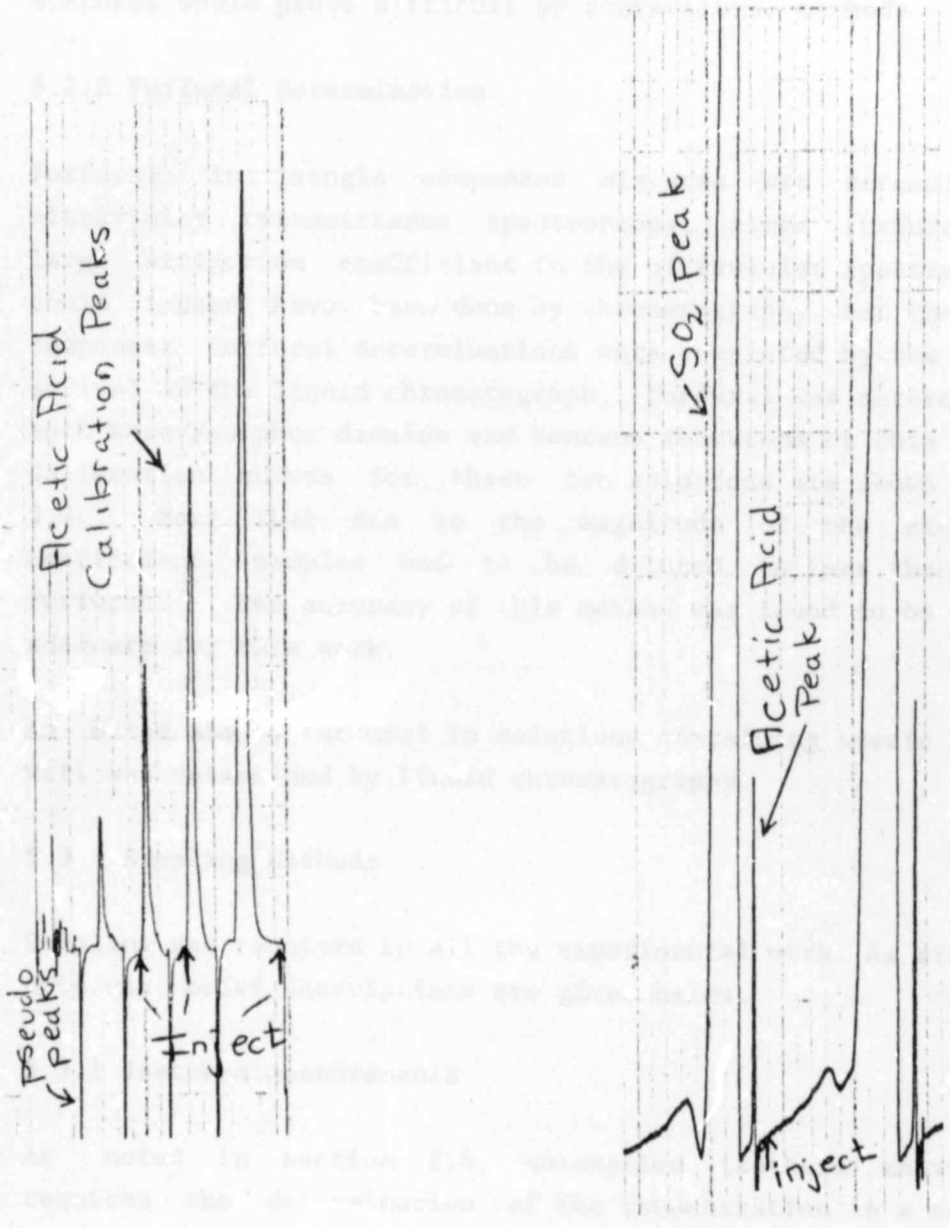

Acetic Acid in water - Calibration Chromatograms

Determination of Acetic Acid in an SO_2 solution

Fig. 5.2

mixtures would prove difficult by conventional methods.

5.2.2 Furfural determination

Furfural in single component mixtures was determined by ultraviolet transmittance spectroscopy, since furfural has a large extinction coefficient in the ultraviolet spectrum. This could indeed have been done by chromatography, but the single component furfural determinations were completed by the date of arrival of the liquid chromatograph. Furfural was determined in both water/sulphur dioxide and benzene solutions by this method. Calibration curves for these two solutions are shown in Fig. 5.3. Note that due to the magnitude of the extinction coefficient, samples had to be diluted to less than 8 mg/l furfural. The accuracy of this method was found to be totally adequate for this work.

As noted above, furfural in solutions containing acetic acid as well was determined by liquid chromatography.

5.3 Sampling Methods

Sampling was required in all the experimental work. As simple as this was, brief descriptions are given below.

5.3.1 Isotherm measurements

As noted in section 2.4, adsorption isotherm measurement requires the determination of the concentration in a solution before and after treatment with a known mass of activated carbon. Sampling the solution before treatment was trivial; a sample of the clear untreated liquid was taken before the addition of activated carbon.

After treatment with activated carbon, the solution was filtered through standard filtering apparatus; samples were taken from the clear filtrate.

UV Spectrophotometer Calibration Curve Fig. 5.3

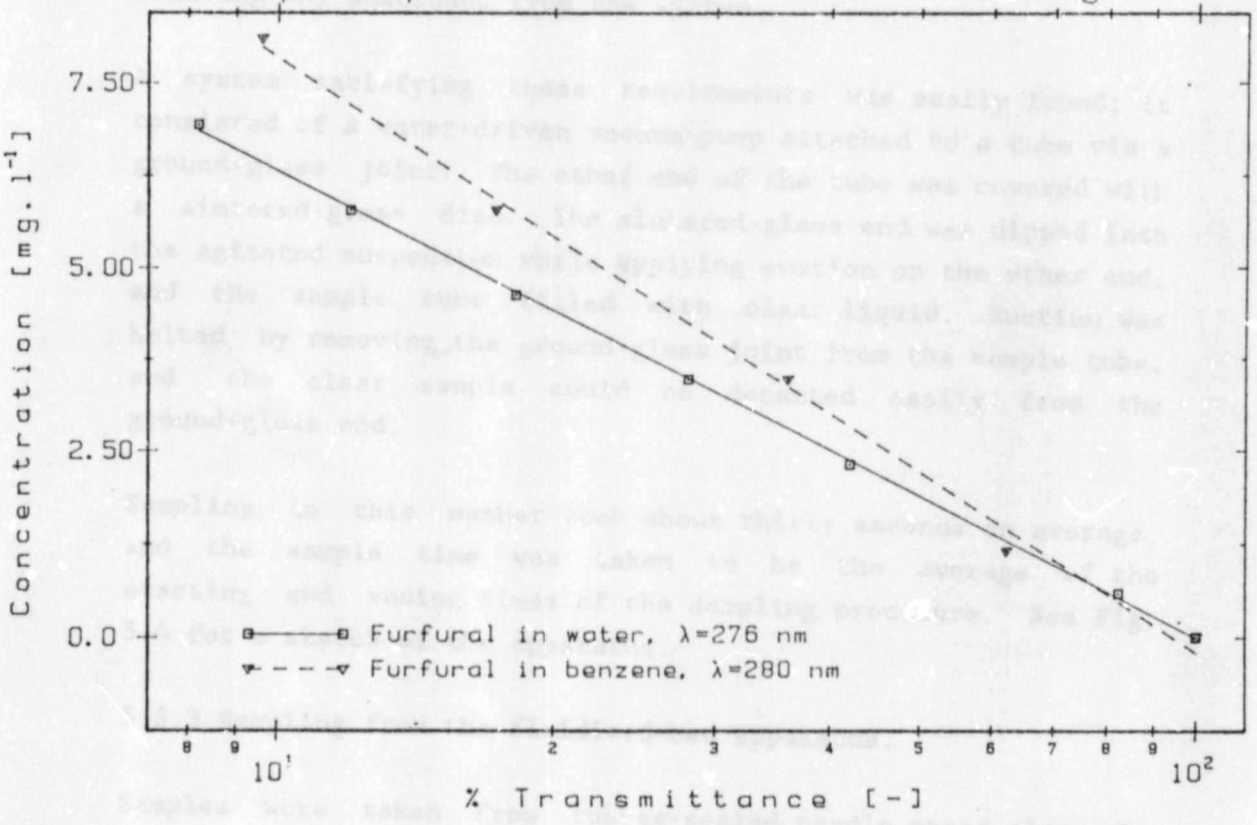

5.3.2 Stirred-tank batch-adsorption tests

Sampling in this case was not as trivial as above, since equilibrium did not exist between the activated carbon and the solution. Thus samples could not be taken into open-necked vessels and then filtered, since this would allow contact of the sample with adsorbent for an undesired, extra length of time. Thus a method had to be used which would allow as rapid a separation of adsorbent and liquid as possible, while not removing any adsorbent from the system.

A system satisfying these requirements was easily found; it consisted of a water-driven vacuum pump attached to a tube via a ground-glass joint. The other end of the tube was covered with a sintered-glass disc. The sintered-glass end was dipped into the agitated suspension while applying suction on the other end, and the sample tube filled with clear liquid. Suction was halted by removing the ground-glass joint from the sample tube, and the clear sample could be decanted easily from the ground-glass end.

Sampling in this manner took about thirty seconds on average, and the sample time was taken to be the average of the starting and ending times of the sampling procedure. See Fig. 5.4 for a sketch of the apparatus.

5.3.3 Sampling from the fluidised-bed apparatus.

Samples were taken from rubber-sealed needle-ports along the height of the bed. Three of these ports were distributed along the upper half of the apparatus, and samples were taken with a syringe and needle from a port within the freeboard, closest to the top of the bed. This ensured a minimum amount of solids in the sample, which was still filtered through a 0.2μm cartridge filter into a sample bottle.

Sketch of Stirred-tank Sampling Apparatus

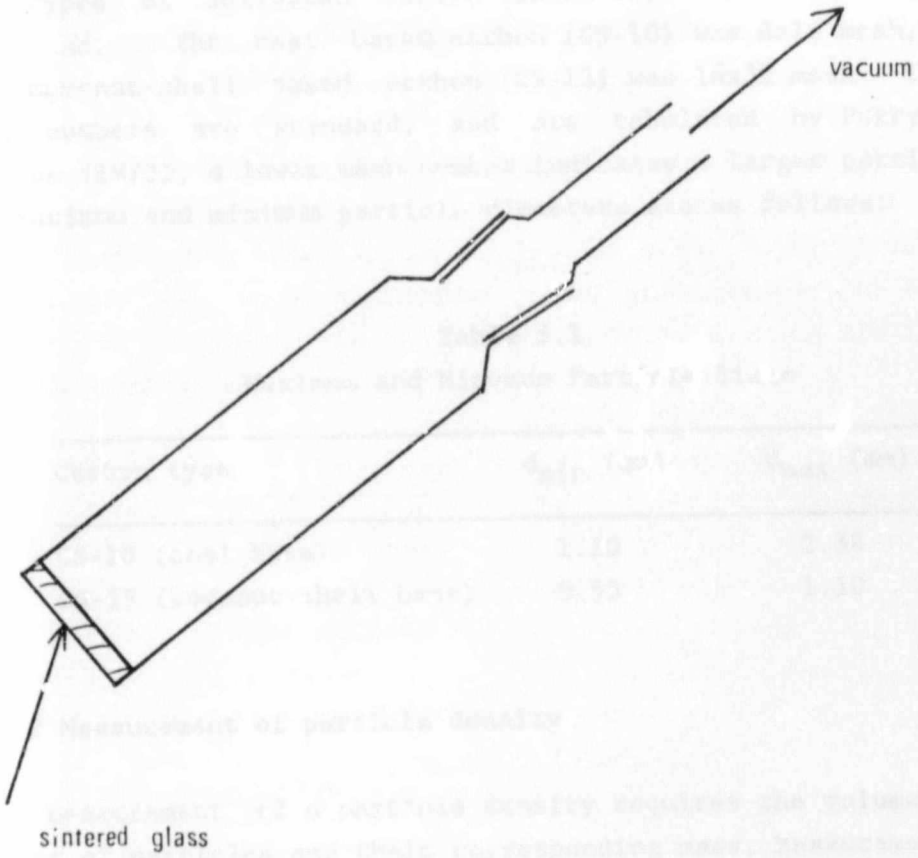

Fig. 5.4

5.4 Measurement of physical properties of the activated carbon

5.4.1 Measurement of average particle size.

The types of activated carbon tested were available in sized fractions. The coal based carbon (CS-10) was 8x16 mesh, and the coconut-shell based carbon (CS-15) was 16x32 mesh. These mesh numbers are standard, and are tabulated by Perry and Chilton (1973); a lower mesh number indicates a larger particle. The maximum and minimum particle diameters are as follows:

Table 5.1
Maximum and Minumum Particle Sizes

Carbon type	d_{min} (mm)	d_{max} (mm)
CS-10 (coal base)	1.10	2.38
CS-15 (coconut-shell base)	0.55	1.10

5.4.2 Measurement of particle density

The measurement of a particle density requires the volume of a number of particles and their corresponding mass. Measurement of the mass of the particles is easy. Measurement of the volume of the particles is not so easy, since the activated carbon is porous, and water poured into a container of activated carbon not only fills the voids between the particles, but also the pores.

Thus a method had to be found to measure the total particle volume, including pore volume. The step-by-step procedure is described below.

1) A known mass of adsorbent W_s was soaked in paraffin for about thirty minutes. This ensured that each particle was thoroughly wetted with the hydrophobic paraffin. This was done

to ensure that water did not soak into the adsorbent.

2) The paraffin was drained off the adsorbent, which was then shaken to remove the excess paraffin.

3) The soaked adsorbent was replaced into the measuring cylinder and the bulk volume of wet adsorbent V_{bulk} was noted.

The measuring cylinder plus wet adsorbent was then weighed, and water was added until level with the top of the adsorbent. The mass, and hence the volume V_{void}, of water required to fill the voids was thus determined. The particle density ρ_s was determined according to the following formula - see **APPENDIX V** for the derivation.

$$\rho_s = \frac{W_s}{V_{bulk} - V_{void}} \qquad \ldots(5/2)$$

Table 5.2
Particle Densities

Carbon type	ρ_s ($kg.m^{-3}$)
CS-10 (coal base)	773.0
CS-15 (coconut shell base)	510.0

5.4.3 Determination of bed-voidage in fluidised-bed experiments

Bed-voidage ϵ had to be determined indirectly. The method used is based on a mass balance and the measured particle densities, see section 5.4.2 above, and takes the form of the following equation - see **APPENDIX V** for the derivation.

$$\epsilon_{bed} = 1 - \frac{W_s}{\rho_s V_{bed}} \qquad \ldots(5/3)$$

where W_s = mass of adsorbent in the bed at any instant [kg]

V_{bed} = volume of the expanded, fluidised bed [m^3]

V_{bed} and ρ_s must be in consistent units.

5.5 Measurement of the variation of bed-voidage with liquid flowrate.

Knowledge of the velocity required to produce fluidisation, and the variation of voidage with flowrate is required to design fluidised beds. The variation of voidage with flowrate was measured for the two types of carbon under consideration. A known mass of adsorbent was placed in the bed. A liquid flowrate through the bed was then selected, and sufficient time was allowed for the expanded bed to reach a steady height. The height was measured and the voidage calculated from eqn.(5/1). The procedure was repeated as necessary.

Results are tabulated below. Experimental measurement commenced at the minimum velocity for onset of fluidisation U_{mf}. For details of the actual measurements and calculations, see APPENDIX V.

Table 5.3

Bed-voidage Variation with Liquid Flowrate

Carbon type CS-10 $U_{mf} \approx 1.8$cm/sec		Carbon type CS-15 $U_{mf} \approx 1.1$cm/sec	
ϵ_{bed} (-)	U_o (cm/sec)	ϵ_{bed} (-)	U_o (cm/sec)
0.53	1.76	0.55	1.11
0.58	2.03	0.62	1.30
0.63	2.38	0.69	1.50
0.66	2.67	0.72	1.67
0.70	3.50*	0.77	1.90
0.74	3.74	0 92	2.24

* Not plotted in Fig.5.5 since result is suspect.

U_o is the velocity with which the liquid would flow if no adsosorbent were present in the vessel. The dependence of bed-voidage on superficial velocity U_o for the two carbon types is plotted in Fig. 5.5.

U_{mf} is a fundamental fluidised-bed design parameter, since no bed with U_o less than this value will fluidise; U_o should ideally be larger than U_{mf}.

Variation of Bed-voidage with Flowrate Fig. 5.5

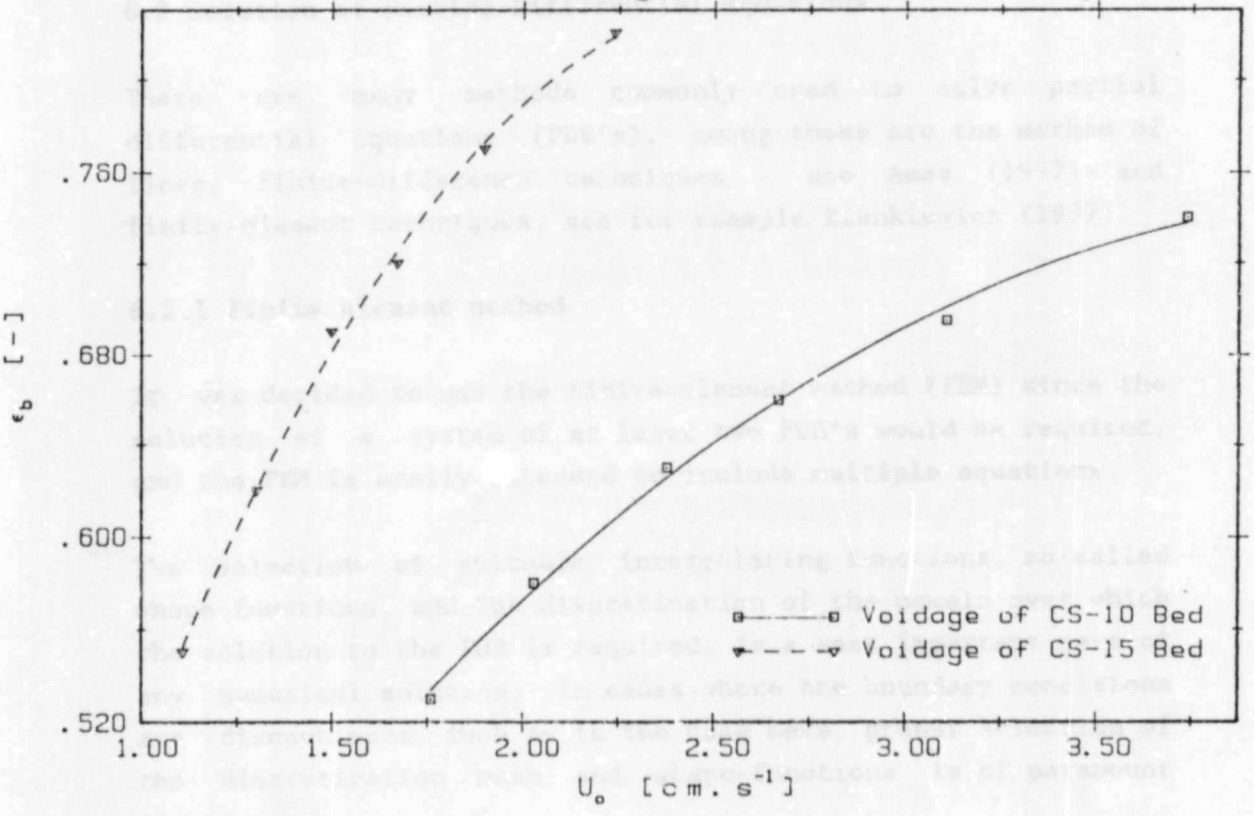

6 NUMERICAL TECHNIQUES

6.1 Introduction

All but two of the models described in section 3.3 require numerical solution. This chapter describes the methods used to solve these equations. Integration of partial differential equations, quadrature and interpolation are discussed.

6.2 Solution of Partial Differential Equations

There are many methods commonly used to solve partial differential equations (PDE's), among these are the method of lines, finite-difference techniques - see Ames (1977)- and finite-element techniques, see for example Zienkiewicz (1977).

6.2.1 Finite element method

It was decided to use the finite-element method (FEM) since the solution of a system of at least two PDE's would be required, and the FEM is easily extended to include multiple equations.

The selection of suitable interpolating functions, so-called shape-functions, and the discretization of the domain over which the solution to the PDE is required, is a most important part of any numerical solution. In cases where the boundary conditions are discontinous, such as is the case here, proper selection of the discretization mesh and shape-functions is of paramount importance.

Many schemes claimed to suppress oscillations due to instability resulting from 'sharp' boundary conditions and largely different coefficients in the PDE's have been proposed. One such method, known as 'upwinding' has been proposed many times in many different forms. However, it has been shown by Gresho and Lee (1981) that 'upwinding' has the same effect as altering terms in the equation and/or the boundary conditions, and they state that the best method of overcoming oscillations is proper

Mesh Used in Numerical Solution of PDE's Fig. 6.1

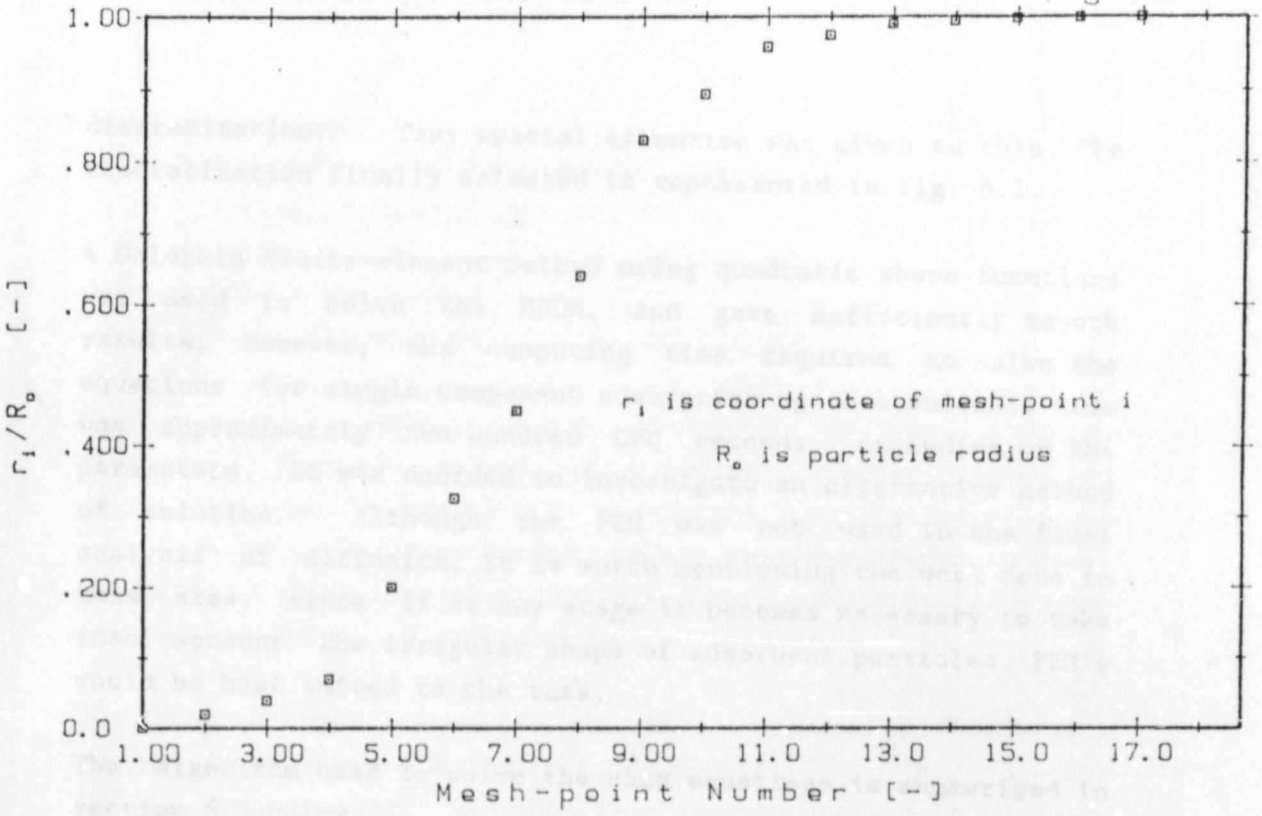

Sample Plot of Adsorption Profile Fig. 6.2

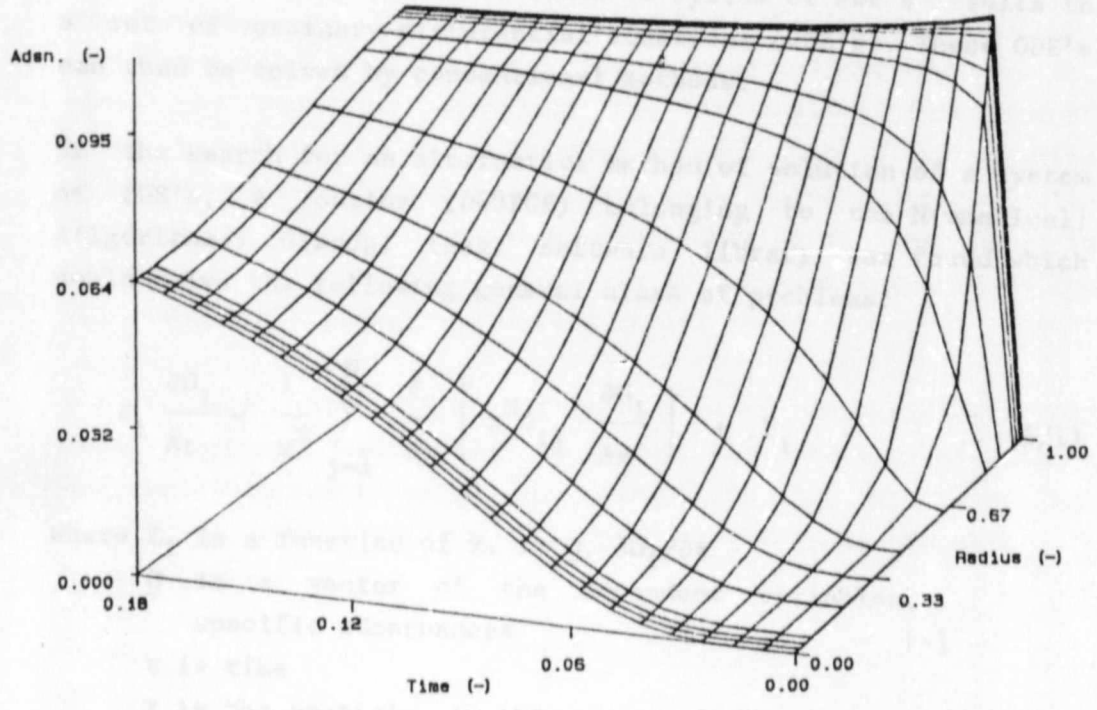

discretization. Thus special attention was given to this. The discretization finally selected is represented in **Fig. 6.1.**

A Galerkin finite-element method using quadratic shape-functions was used to solve the HSDM, and gave sufficiently smooth results. However, the computing time required to solve the equations for single component adsorption up to a suitable time was approximately two-hundred CPU seconds, depending on the parameters. It was decided to investigate an alternative method of solution. Although the FEM was not used in the final analysis of diffusion, it is worth mentioning the work done in this area, since if at any stage it becomes necessary to take into account the irregular shape of adsorbent particles, FEM's would be best suited to the task.

The algorithm used to solve the HSDM equations is summarised in section 6.5 below.

6.2.3 The method of lines

Application of the method of lines to system of PDE's results in a set of ordinary differential equations (ODE's). These ODE's can then be solved by conventional methods.

In the search for an alternative method of solution of a system of PDE's, a routine (D03PGE) belonging to the N(umerical) A(lgorithms) G(roup) (Nag) software library was found which could solve the following general class of problems:

$$E_i \frac{\partial \Omega_i}{\partial t} = \frac{1}{x^M} \sum_{j=1}^{N} \frac{\partial}{\partial x} \left[x^M G_{ij} \frac{\partial \Omega_i}{\partial x} \right] + P_i \qquad \ldots(6/1)$$

where E_i is a function of x, t, $\underline{\Omega}$, $\partial\Omega_i/\partial t$

$\underline{\Omega}$ is a vector of the dependent variables, specific adsorbances [-]

t is time

x is the spatial-, in this case radial-,

coordinate. [m]

M is the 'coordinate-system' parameter.
For spherical coordinates M = 2 [-]

N is number of equations in the system.

G_{ij} is a function of x, t, $\underline{\Omega}$

P_i is a function of x, t, $\underline{\Omega}$, $\partial\Omega_i/\partial t$

The routine supports boundary conditions of the Dirichlet (specified function values at boundary), Cauchy (specified derivatives at boundary) or mixed type. Coefficients of the terms in the boundary conditions may have dependence on time, position or function value. These boundary condition facilities are comprehensive and are adequate for this work.

The routine uses the method of lines to reduce the PDE's to a system of ODE's, and then uses Gear's method to integrate the ODE's. This package is ideally suited to systems of PDE's in spherical coordinates, and expansion to more components in the solution would be a matter of altering a few parameters in the argument list.

The routine was implemented to solve the HSDM equations. Implementation required more than merely calling the routine, since the boundary conditions are not explicit functions of time, but have to be calculated at each step of the solution procedure by application of a mass-balance. Computer time required to solve a problem comparable to that mentioned in section 6.2.2 was about a fifth of the time required by the FEM. Thus this package is better in all respects.

Due to the large difference in complexity between single- and multi-component adsorption isotherms, the programs for single- and multicomponent adsorption simulation are separate. The algorithm used to solve the HSDM equations is summarised in section 6.5.

6.3 Quadrature

As can be seen on examination of the HSDM equations in section 3.3, quadrature of the specific adsorbance profile in the adsorbent particle is required to calculate the variation in liquid-phase concentration. This was done by Cautious Adaptive Romberg Integration, as implemented in the I(nternational) M(athematical) and S(tatistical) software L(ibrary) (IMSL) routine 'DCADRE'. The routine calculates successive approximations to the integral using different step-sizes, and then performs Romberg extrapolation to improve the estimate. When the estimated error is less than a user-supplied tolerance, the answer is returned.

6.4 Interpolation

Since the numerical solution to the PDE returned by routine D03PGE consists of a set of discrete values, it was necessary to interpolate these values to perform quadrature on the profile. This was done using simple linear interpolation, and the results were found to be sufficiently accurate. The selection of linear interpolation constitutes a large saving in computer time, since the interpolation routine is called hundreds of times by the quadrature routine DCADRE.

6.5 The Algorithm for the Solution of the System of PDE's

The algorithm is summarised below.

1) After reading in data on system volume, mass of adsorbent, and initial concentrations, calculate the parameters used to convert the problem into dimensionless form - see section 4.4 for details. These parameters are imbedded into the adsorption isotherm routine so that values of adsorbance returned are in dimensionless, reduced form.

2) Read in the particle discretization data, and set the dimensionless initial conditions at each point.

3) Using the liquid-phase concentrations, calculate the dimensionless specific adsorbances at the particle exterior.

4) Call the PDE solution routine **D03PGE** to integrate the equations to the new time-value. The routine returns the specific adsorbances of each component at each of the discretization points at the new time value.

5) Calculate the integral in eqn.(4/7) for each component using **DCADRE**. Hence calculate the new liquid-phase concentrations for each component.

6) Calculate the derivatives of the specific adsorbances of each component at the particle exterior. Hence calculate the flux into each particle.

Repeat the procedure 2) to 6) until the required time-value is reached.

Notes

- In the case of rate-calculations, which are done for constant liquid-phase concentrations, step 5) is omitted.
- The time-step used must be small enough so that the decrease in liquid-phase concentration is small enough not to cause stability problems in the next cycle of the solution procedure.

A FORTRAN 77 program was written to implement the above algorithm. The program used to solve the single-component equation is similar, and is not included. A listing of the program may be found in **APPENDIX II**.

6.6 Simulation Results

A three-dimensional sample plot of a calculated adsorbance profile for single adsorption is shown in **Fig. 6.2**. Calculated concentration histories may be found in abundance in section 4.6.

7 FLUIDISED BED ADSORBERS

7.1 Introduction

A major advantage of fluidised-bed operations is that the fluidised solids are mobile and may thus easily be transported for processing. In the case of adsorption operations, the adsorbent could be continuously removed from the bottom of the bed and regenerated by some means, while feeding regenerated adsorbent to the top of the bed, thus constituting a continuous, steadt-state process. The advantage of operating in this fashion is that effluent quality is constant, and that only a small fraction of adsorbent in the bed is highly loaded; time-average adsorption rates are thus higher than in batch-solids operations, and equipment dimensions correspondingly smaller.

The alternative is packed-column operation, which would result in effluent of varying quality and the need for at least a pair of columns, one of which would be operating while the other was being regenerated. This sort of operation is not ideal, and thus the fluidised mode of operation has been selected.

This chapter deals with the design of a two-component fluidised bed adsorber. Consideration is given to the fluidisation characteristics of the two adsorbent types and variation of adsorption rates with adsorbent residence time. Special consideration is given to the dependence of the extents of adsorption of the two components, and the effect that the presence of two components has on the rate of adsorption of each.

7.2 The Equations Describing Fluidised-bed Adsorption

The full equations describing any continuous fluidisation operation need to account for imperfect mixing and a distribution of particle 'ages' in the bed, as Muratov, Protod'yakanov and Romankov (1979) have done. However, a glance at the above reference showed that the full treatment would be

too time consuming for the purpose in mind. It was decided to simplify the treatment by making some simple assumptions.

7.2.1 Basic assumptions

1) The fluidised adsorbent was assumed to be perfectly mixed. Although this assumption does not usually hold, it considerably simplifies the mathematical treatment, and it is not totally unrealistic. Observation of both types of adsorbent fluidised at liquid-velocities sufficiently above minimum fluidisation velocity showed the solid particles to be well-mixed.

Apart from validating the design equations, proper fluidisation ensures efficient operation of any fluidised-bed operation by eliminating bypassing. See section 5.4.3 for details of the fluidisation behaviour of the two types of adsorbent.

2) The liquid was assumed to be in 'plug-flow' through the fluidised adsorbent. This is a simplification, since the adsorbent particles which move rapidly up and down in a fluidised-bed are sure to 'drag' a film of liquid around with them, thus causing a large degree of liquid phase back-mixing. This assumption considerably simplifies the mathematical treatment of the equations.

3) Since proper modelling of adsorption rates in a fluidised-bed would entail statistical modelling of the time-varying concentration that a particular particle 'sees' during its stay in the bed, it was assumed that the rate of adsorption could be characterised by some average liquid-phase concentration. The rate of adsorption is calculated from the residence-time distribution of the solids (which are assumed to be perfectly mixed) and the segregated mixing model, as described in section 7.5

7.2.2 The simplified equations

Under the above assumptions, the equations describing adsorption

in a fluidised bed may be written as follows:

$$\frac{\partial C_{f,i}(z,t)}{\partial z} = -\frac{\epsilon_b}{U_o}\frac{\partial C_{f,i}(z,t)}{\partial t} - \frac{r_{a,i}(\hat{\underset{\sim}{C}},\tau_s)(1-\epsilon_b)\rho_s S_w}{U_o} \qquad \ldots(7/1)$$

$$C_{f,i}(0,t) = C_{feed,i}(t) \qquad \ldots(7/2)$$

$$C_{f,i}(z,0) = 0 \qquad 0 < z < h_b \qquad \ldots(7/3)$$

where subscript f refers to bulk fluid properties of component i

subscript feed refers to feed concentration

subscript b refers to bed properties

z = distance along bed in direction of flow [m]

h_b = height of fluidised bed [m]

$r_{a,i}$ = rate of adsorption of component i [$kg.m^{-2}.s^{-1}$]

S_w = specific external surface area of adsorbent [$m^2.kg^{-1}$]

$\hat{\underset{\sim}{C}}$ = vector of average liquid-phase concentrations. See section 7.2.1 [$kg.m^{-3}$]

τ_s = average residence time of adsorbent [s]

Other symbols as previously defined.

See **APPENDIX VI** for the derivation of **eqn.(7/1)** and boundary conditions

For the particular case of interest where the rate of adsorption is determined by the intraparticle diffusion, as discussed in section 3.3.2, the instantaneous rate of adsorption at time $\hat{t}$ may be calculated as follows:

$$r_{a,i}(\hat{\underset{\sim}{C}}, \hat{t}) = \frac{\rho_s D^*_{s,i} \exp(\beta_i \Theta_i) \theta^*}{r_o} \left. \frac{\partial \Theta_i(\xi, t)}{\partial \xi} \right|_{\xi=1} \quad \ldots(7/4)$$

Note

- The function Θ_i on the right hand side of eqn.(7/4) has been transformed back into the time-domain.
- The second term on the right-hand side of eqn.(7/4) is the instantaneous rate of adsorption, and is calculated as the rate of adsorption by a particle of adsorbent which has been exposed to a solution of concentrations $\hat{\underset{\sim}{C}}$ for a length of time $\hat{t}$.
- Since the Θ_i depend on the liquid-phase concentrations of all components, the rate of adsorption of component i depends also on the liquid-phase concentrations of all the other components.
- In the case of steady-state continuous operation, the effective rate of adsorption is calculated using the segregated mixing model and the adsorbent residence-time distribution - see section 7.5 - and is assumed constant for any given set of average concentrations $\hat{\underset{\sim}{C}}$ and any given solids residence time τ_s.
- In the case of batch-solids operations, the rate of adsorption is identical to the instantaneous rate of adsorption, since all particles have the same 'age'.

From the above notes, it is clear that the modelling of a fluidised-bed adsorber requires the simultaneous solution of the fluidised bed equations, eqn.(7/3), and the intraparticle diffusion equations, eqn.(3/7) with boundary conditions described in section 3.3.2.

7.3 Calculation of the Rates of Adsorption

As discussed in Notes above, the rates of adsorption for given average concentrations and mean adsorbent residence times are constants under the assumptions made. Thus if the average concentrations are known in advance, the design of a fluidised bed adsorber by this method is greatly simplified.

7.3.1 The average concentrations

The average concentration was defined as the arithmetic-average concentration, thus:

$$\hat{C}_{f,i}(t) = \frac{C_{feed,i} + C_{ex,i}}{2} \qquad \ldots(7/5)$$

Where subscript ex refers to exit concentration.

7.4 Unsteady-state Operation of a Fluidised-bed Adsorber

Due to the extreme difficulty and expense of building an adsorber with continuous supply and extraction of adsorbent, it was necessary to perform tests on an adsorber in which the fluidised adsorbent was a batch-phase, while fresh liquid was continuously passed through the bed. It was hoped that comparison between simulated performance and experimental measurements would help to clarify the validity of the design procedure. Thus a model of this situation was developed.

7.4.1 Development of a simple unsteady-state model

Some simple assumptions regarding the rate of adsorption can simplify the still complicated analysis required to simulate this system. It is clear that there is no interest in the behaviour of such a semi-batch system after extended periods of operation. Thus a model was developed which holds for low extents of adsorption.

The propagation of a 'front' of solute up the height of the bed is to be expected. The rates of adsorption in the region between the feed-point and the 'front' are governed by the some concentration between the feed and effluent concentrations, $\hat{C}$, and (since the adsorbent is a batch phase) the 'age' t' of the adsorbent, i.e. the time since the start of the run.

Note that for a batch-solids operation there is no distribution of residence times for the adsorbent particles. Thus:

$$r_{a,i} = r_{a,i}(\hat{\underset{\sim}{C}}, t') \qquad \ldots(7/6)$$

Where the calculation of the rate is as described in 7.2.2 above.

Thus the equation and boundary conditions may be written as follows:

$$\frac{\partial C_{f,i}(z,t)}{\partial z} = -\frac{\epsilon_b}{U_o}\frac{\partial C_{f,i}(z,t)}{\partial t} - \Psi_i \qquad \ldots(7/7)$$

$$C_{f,i}(0,t) = C_{feed,i} \qquad \ldots(7/8)$$

$$C_{f,i}(z,0) = 0 \qquad 0 < z < h_b \qquad \ldots(7/9)$$

Where $\Psi_i = \dfrac{r_{A,i}(\hat{\underset{\sim}{C}}, t')(1-\epsilon_b)\rho_s S_w}{U_o}$

Note that Ψ_i is considered constant here.

7.4.2 Solution of the simple unsteady-state model equations

Eqn.(7/7) was solved for a single component by a boundary-layer technique; the section of the bed between the feedpoint and the advancing solute 'front' was considered as the boundary-layer. The boundary-layer solution may be written as follows:

$$\frac{C(z,t)}{C_{feed}} = 1 - 1.5\eta(z,t) + 0.5\left[\eta(z,t)\right]^3 = \varphi\left(\eta(z,t)\right) \qquad 0 < \eta < 1 \qquad \ldots(7/10)$$

where $\eta(z,t) = \frac{z}{\delta(t)}$

$$\delta(t) = \frac{M}{\psi}\left[e^{-\psi U_o t/(\epsilon_b L)} - 1\right]$$

$$M = \varphi(1) - \varphi(0) \qquad L = \int_0^1 \varphi(\eta)\,d\eta \qquad \psi = \frac{\Psi}{C_{feed}}$$

Note that Ψ (and hence ψ) is a decreasing function of time.

An assumption inherent in this model is that the bed is short, since the model assumes that all adsorbent has the same 'age', i.e. has been exposed to the solution for the same time. Thus the time to 'breakthrough' must be relatively short so that all adsorbent is wetted with the solution as soon as possible.

This equation may be used to simulate the unsteady-state operation of the batch fluidised-bed adsorber described in section 7.4 above. For details of the boundary-layer solution, see APPENDIX VI.

7.4.3 Experimental results

The batch fluidised-bed adsorber was run for each combination of adsorbent and solute; the results are presented below.

Results for Carbon Type CS-10

The results for fluidised-bed adsorption of acetic acid and furfural onto CS-10 are summarised in Table 7.1 below:

Table 7.1

Unsteady-state Fluidised-bed Adsorber Experiments on CS-10

		Acetic Acid	Furfural
C_{feed}	[$kg.m^{-3}$]	4.24	8.2
U_o	[$cm.s^{-1}$]	2.6	2.4
h_b	[m]	0.40	0.41
ϵ_b	[-]	0.7	0.7
W_s	[kg]	0.632	0.600

t [s]	$C(t)/C_{feed}$ [-]	t [s]	$C(t)/C_{feed}$ [-]
33	0.588	13	0.618
59	0.769	28	0.688
180	0.883	48	0.722
259	0.904	78	0.789
383	0.934	168	0.827
443	0.942	198	0.864
522	0.963	288	0.892
561	0.963	408	0.923

The results tabulated above are plotted in Figs.7.1 and 7.2 respectively. Details of the experimental techniques may be found in section 5.3.2.

Results for Carbon Type CS-15

The results for fluidised-bed adsorption of acetic acid and furfural onto CS-15 are summarised in Table 7.2 below:

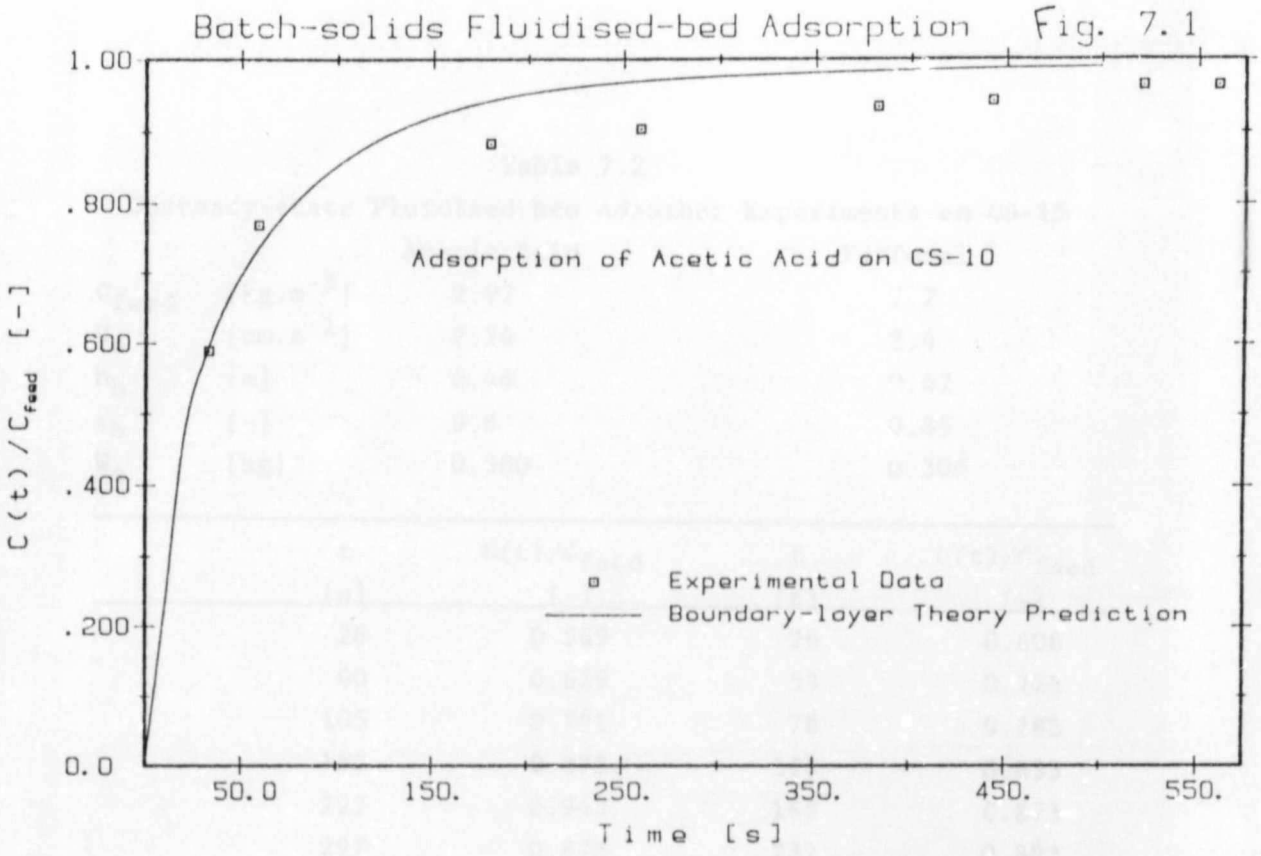
Batch-solids Fluidised-bed Adsorption Fig. 7.1
1.00
.800
.600
.400
.200
0.0
C(t) / C feed [-]
Adsorption of Acetic Acid on CS-10
Experimental Data
Boundary-layer Theory Prediction
50.0
150.
250.
350.
450.
550.
Time [s]

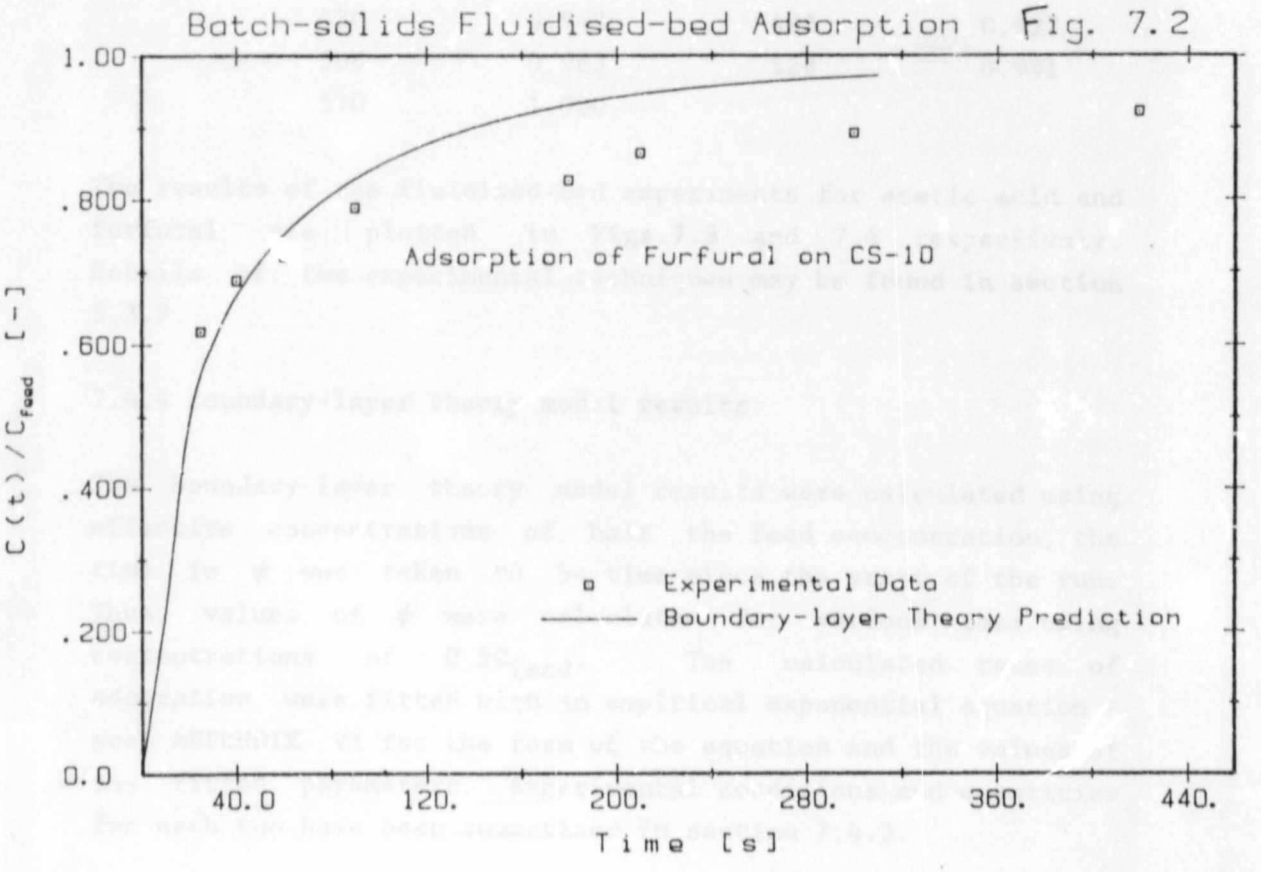
Batch-solids Fluidised-bed Adsorption Fig. 7.2
1.00
.800
.600
.400
.200
0.0
C(t) / C feed [-]
Adsorption of Furfural on CS-10
Experimental Data
Boundary-layer Theory Prediction
40.0
120.
200.
280.
360.
440.
Time [s]

Table 7.2

Unsteady-state Fluidised-bed Adsorber Experiments on CS-15

		Acetic Acid	Furfural
C_{feed}	[$kg.m^{-3}$]	2.97	7.2
U_o	[$cm.s^{-1}$]	2.24	2.4
h_b	[m]	0.44	0.47
ϵ_b	[-]	0.8	0.85
W_s	[kg]	0.300	0.300

t [s]	$C(t)/C_{feed}$ [-]	t [s]	$C(t)/C_{feed}$ [-]
26	0.569	26	0.608
60	0.639	53	0.728
105	0.791	78	0.785
159	0.872	118	0.833
227	0.943	168	0.873
297	0.878	237	0.893
367	0.902	318	0.905
430	0.943	408	0.927
508	0.963	528	0.931
570	1.000		

The results of the fluidised-bed experiments for acetic acid and furfural are plotted in Figs.7.3 and 7.4 respectively. Details of the experimental techniques may be found in section 5.3.2.

7.4.4 Boundary-layer theory model results

The boundary-layer theory model results were calculated using effective concentrations of half the feed concentration; the time in ψ was taken to be time since the start of the run. Thus, values of ψ were calculated for various times using concentrations of $0.5C_{feed}$. The calculated rates of adsorption were fitted with an empirical exponential equation - see APPENDIX VI for the form of the equation and the values of the fitted parameters. Experimental conditions and quantities for each run have been summarised in section 7.4.3.

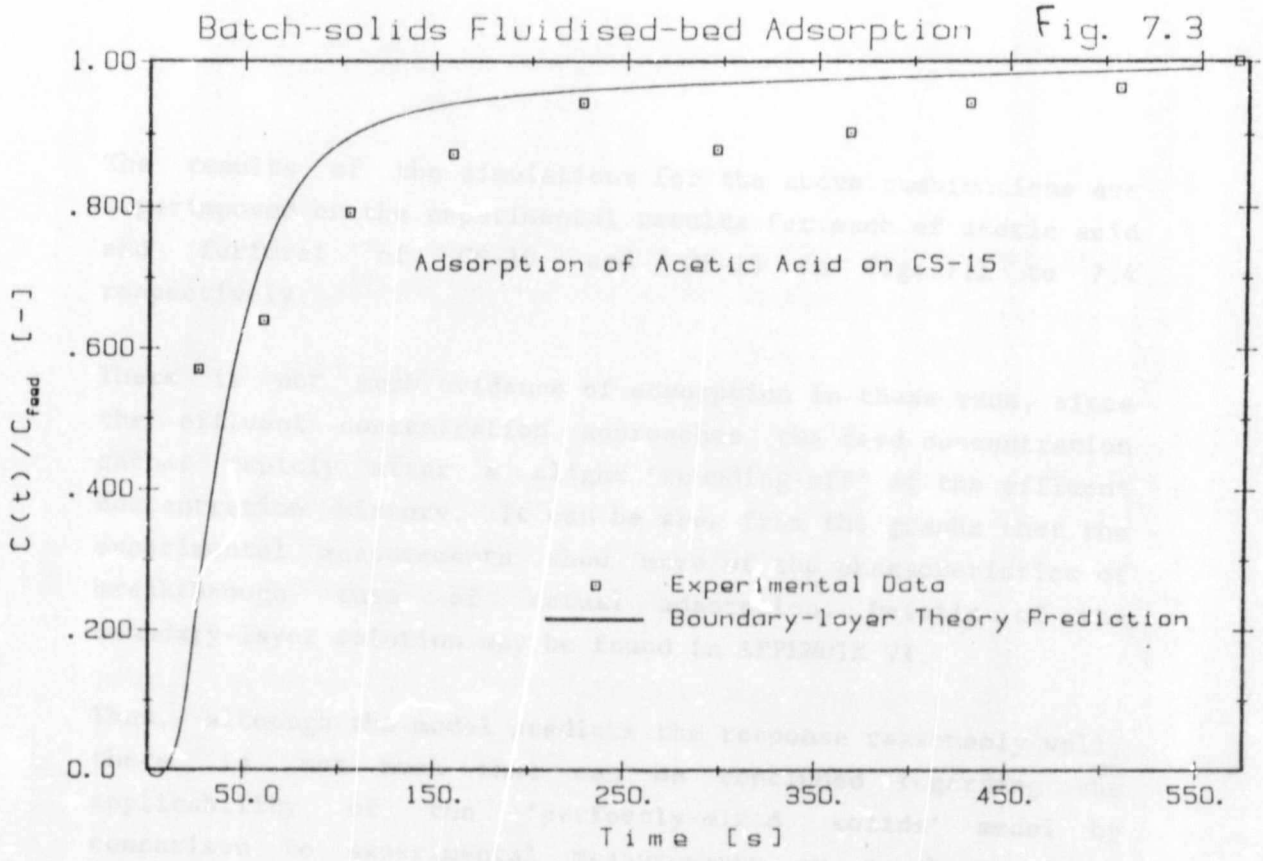
Batch-solids Fluidised-bed Adsorption Fig. 7.3
1.00
.800
.600
.400
.200
0.0
C(t) / C feed [-]
Adsorption of Acetic Acid on CS-15
Experimental Data
Boundary-layer Theory Prediction
50.0
150.
250.
350.
450.
550.
Time [s]

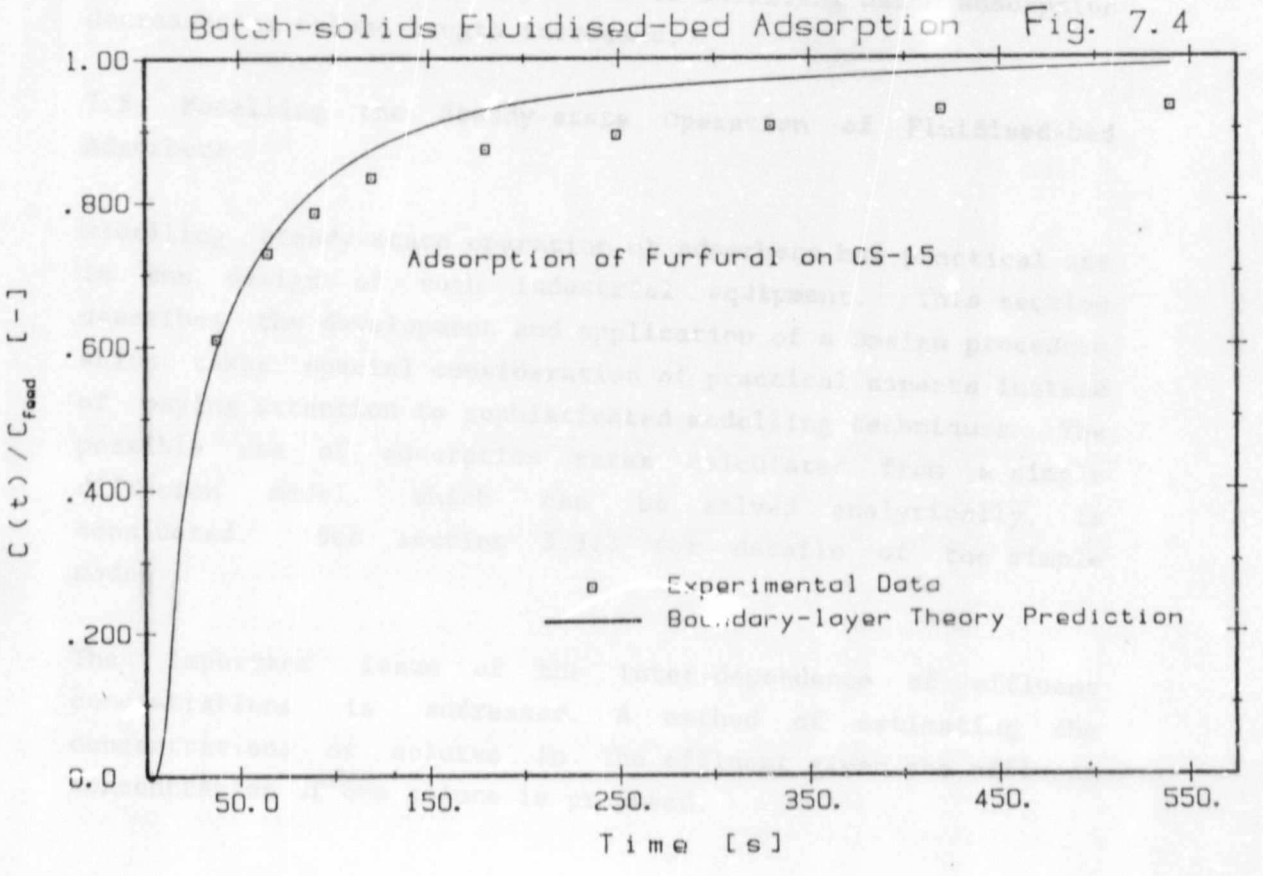
Batch-solids Fluidised-bed Adsorption Fig. 7.4
1.00
.800
.600
.400
.200
0.0
C(t) / C feed [-]
Adsorption of Furfural on CS-15
Experimental Data
Boundary-layer Theory Prediction
50.0
150.
250.
350.
450.
550.
Time [s]

The results of the simulations for the above combinations are superimposed on the experimental results for each of acetic acid and furfural of CS-10 and CS-15 in Figs.7.1 to 7.4 respectively.

There is not much evidence of adsorption in these runs, since the effluent concentration approaches the feed concentration rather rapidly after a slight 'rounding-off' of the effluent concentration history. It can be seen from the graphs that the experimental measurements show more of the characteristics of breakthrough than of actual adsorption. Details of the boundary-layer solution may be found in APPENDIX VI.

Thus, although the model predicts the response reasonably well, there is not much that can be concluded regarding the applicability of the 'perfectly-mixed solids' model by comparison to experimental measurements on a short column. Unfortunately, as discussed in section 7.4.2, the suitability of the boundary-layer theory model to modelling batch adsorption decreases as column length increases.

7.5 Modelling the Steady-state Operation of Fluidised-bed Adsorbers

Modelling steady-state operation of adsorbers has practical use in the design of such industrial equipment. This section describes the development and application of a design procedure which takes special consideration of practical aspects instead of paying attention to sophisticated modelling techniques. The possible use of adsorption rates calculated from a simple diffusion model, which can be solved analytically, is considered. See section 3.3.3 for details of the simple model.

The important issue of the inter-dependence of effluent concentrations is addressed. A method of estimating the concentrations of solutes in the effluent given the effluent concentration of one solute is proposed.

The assumptions used in the modelling of steady-state fluidised-bed adsorption are discussed in section 7.2.1 .

7.5.1 The model equations

The model equations for a steady-state fluidised-bed adsorber may be obtained by removing any time dependence from eqn.(7/7) and the attendant boundary and initial conditions (7/8) and (7/9). The resulting equation is as follows:

$$\frac{\partial C_{f,i}(z)}{\partial z} = -\hat{\Psi}_i \qquad \ldots(7/11)$$

$$C_{f,i}(0) = C_{feed,i} \qquad \ldots(7/12)$$

$$\text{Where } \hat{\Psi}_i = \frac{\hat{r}_{a,i}(\hat{\underset{\sim}{C}}, \tau_s)(1-\epsilon_b)\rho_s S_w}{U_o} \qquad \ldots(7/13)$$

$$\hat{r}_{a,i}(\hat{\underset{\sim}{C}}, \tau_s) = \int_0^\infty I(t) r(\hat{\underset{\sim}{C}}, t)\, dt = \int_0^\infty \left\{ \frac{e^{-t/\tau_s}}{\tau_s} \right\} r(\hat{\underset{\sim}{C}}, t)\, dt \qquad \ldots(7/14)$$

Where $I(t)$ is the internal age density function of the adsorbent, and other symbols are as defined above. It has been assumed here that the instantaneous rate of adsorption is a unique function of time.

Eqn.(7/14) is derived in APPENDIX VI.

7.5.2 Solution of the steady-state model equations

Under the simplifying assumptions discussed in section 7.2.1

above, the function $\hat{\Psi}_i$ depends only on the mean residence-time of the adsorbent and the average concentration of each component in the bed. The solution to the system of equations eqn.(7/11) appears to be almost trivial, and indeed it is, with one provision: the effluent concentrations may not be chosen or determined independently. The reason for this is that rates of adsorption are dependent on all concentrations through the average concentration vector $\hat{\underline{C}}$, as discussed above. A procedure for estimating the dependent effluent concentrations in a two component system is proposed in section 7.5.4 .

Bearing this restriction in mind, the solution to the system of ordinary differential equations (7/11) with boundary conditions (7/12) is easily obtained:

$$C_{f,i}(h) = C_{feed,i} - \hat{\Psi}_i h_b \qquad \ldots(7/15)$$

As usual, simplifying assumptions as discussed above limit the applicability of the solution to reality. The limitation in this case is that eqn.(7/15) only approximates the behaviour of a fluidised-bed adsorber, since the variation up the bed of liquid-phase concentration has not been accounted for.

Eqn.(7/15) would be best used for cases in which the highest extent of adsorption $C_{feed,i}-C_{ex,i}$ is not too large.

7.5.3 Determination of a consistent set of effluent concentrations

As mentioned above, since the rates of adsorption are inter-dependent, the effluent concentrations are also inter-dependent. In this section a method of quickly estimating one effluent concentration in a two component system given the other concentration is proposed.

In a two component system, there are two equations of the form of eqn.(7/11). Division of one equation by the other yields